

A Note on Newton-Like Iterative Solver for Multiple View L2 Triangulation

*

Abstract

In this paper, we show that the L2 optimal solutions to most real multiple view L2 triangulation problems can be efficiently obtained by two-stage Newton-like iterative methods, while the difficulty of such problems mainly lies in how to verify the L2 optimality. Such a working two-stage bundle adjustment approach features the following three aspects: first, the algorithm is initialized by *symmedian point* triangulation, a multiple-view generalization of the mid-point method; second, a symbolic-numeric method is employed to compute derivatives accurately; third, globalizing strategy such as line search or trust region is smoothly applied to the underlying iteration which assures algorithm robustness in general cases.

Numerical comparison with *fnl* method shows that the *local* minimizers obtained by the two-stage iterative bundle adjustment approach proposed here are also the L2 optimal solutions to all the calibrated data sets available online by the Oxford visual geometry group. Extensive numerical experiments indicate the bundle adjustment approach solves more than 99% the real triangulation problems optimally. An IEEE 754 double precision C++ implementation shows that it takes only about 0.205 second to compute all the 4983 points in the Oxford *dinosaur* data set via Gauss-Newton iteration hybrid with a line search strategy on a computer with a 3.4GHz Intel® i7 CPU.

Keywords: Triangulation; L2 optimality; iterative methods; line search; trust region.

1 Introduction

Triangulation is a critical topic in computer vision with applications in 3D object reconstruction, map estimation, robotic path-planning, surveillance and virtual reality [4, 11, 12, 24]. Efficient two-view triangulation methods [15, 29] and especially multiple-view L2 optimal ones [3, 4, 16, 25] have drawn intensive research interests; the latter give rise to favorable maximum likelihood estimates under the assumption of independent gaussian noises [12] but still remain not well-resolved.

Triangulation algorithms which guarantee L2 optimality for up to three-view cases are mainly based on polynomial solving, symbolic-numeric Gröbner basis methods in solving polynomial systems, and branch-and-bounds optimization techniques [3, 12, 16, 25]. Recent research indicates that such an algorithm as can find a closed-form n -view L2 optimal solution does not exist [11].

*correspondence author

A novel non-iterative method based on fundamental matrix and linear matrix inequalities, *tfml*, by Chesi et al [4], is efficient and able to handle more than three-view L2 triangulation. The major limitations of *tfml* might be the low solution accuracy in the *conservative cases* [4] and the fast efficiency decline due to scale increasing of the converted eigen value problem(EVP) when the number of cameras increases. Despite of these, *tfml* is probably by far the most successful n -view L2 triangulation method created naturally with a *necessary and sufficient* criterion for L2 optimality verification [4,11] and will be used as benchmark here.

Traditional iterative methods such as the bundle adjustment optimization via Levenberg-Marquardt are mainly criticized for their no ideal initialization and the possible local convergence issue [3, 11, 13, 16, 25, 28]. As far as we know, none of the state-of-the-art triangulation approaches which asserts L2 optimality for multiple view triangulation are iterative methods. Recent publications indicate that *bundle adjustment* optimization performs poorer than even some of the suboptimal methods [23, 24].

We find most of the real n -view L2 triangulation problems don't have the difficulty of multiple local minima, i.e., in most cases the global L2 optimal solutions can be approached by solving only a convex problem via simple Newton-like methods [11]. As a matter of fact, a lot of the most cited real data sets can be globally solved by iterative methods with excellent accuracy and high efficiency. These data sets include but are not limited to *dinosaur*, *model house*, *corridor*, *Merton colleges I, II and III*, *University library* and *Wadham College*, which are made available online by the visual geometry group of Oxford university(VGG, <http://www.robots.ox.ac.uk/~vgg/data/data-mview.html>) and are widely used to evaluate new triangulation algorithms.

In our numerical experiments, Newton-Raphson, Gauss-Newton and Levenberg-Marquardt methods all work successfully on Oxford VGG data when being implemented by:

- (1) initializing via *symmedian-point* triangulation to obtain a good start point;
- (2) computing all derivatives, gradients and Hessians of the cost function included, via a symbolic-numeric approach (or multiple precision computation) to assure high accuracy;
- (3) using Newton-like underlying iterative methods such as Newton-Raphson, Gauss-Newton and other variants, smoothly hybrid with globalizing strategies in order to handle hard cases when symmedian point is not a good start point.

In this work we will show these implementation details and briefly introduce some criteria useful in verifying the L2 optimality [4, 11, 22]. We intend to present that bundle adjustment optimization with appropriate implementation details is a practically well-performed approach in solving the multiple-view L2 triangulation problems.

2 Implementation details of the iterative solver

The cost function of a typical unconstrained least square problem has the following form [18]:

$$\frac{1}{2}f(X) = \frac{1}{2}r(X)^T r(X) = \frac{1}{2} \sum_{i=1}^m \phi_i^2(X) \quad (2.1)$$

The n -view L2 triangulation is the least square problem as in (2.2): given n pinhole cameras P_i in 3×4 and n 2D image homogenous coordinates $\mathbf{x}_i = (u_i, v_i, 1)^T$, find the global least square minimizer X^* :

$$X^* = \arg \min_{X \in \mathbb{R}^3} f(X) = \arg \min_{X \in \mathbb{R}^3} \sum_{i=1}^n \|\mathbf{x}_i - \hat{\mathbf{x}}_i\|_2^2, \quad \text{where } \hat{\mathbf{x}}_i = (\hat{u}_i, \hat{v}_i, 1)^T = \frac{P_i}{\lambda_i} X^\ominus, i = 1 \cdots n. \quad (2.2)$$

$X = (x, y, z)^T$ represents a 3D scene point, $X^\ominus = (x, y, z, 1)^T$ is X in homogeneous coordinates and λ_i is the projective depth corresponding to P_i .

The projection of n -camera cases can be represented as in equation (2.3):

$$\begin{bmatrix} \lambda_1 u_1 \\ \lambda_1 v_1 \\ \lambda_1 \\ \lambda_2 u_2 \\ \lambda_2 v_2 \\ \lambda_2 \\ \vdots \\ \lambda_n u_n \\ \lambda_n v_n \\ \lambda_n \end{bmatrix} = \begin{bmatrix} p_{11}^1 & p_{12}^1 & p_{13}^1 & p_{14}^1 \\ p_{21}^1 & p_{22}^1 & p_{23}^1 & p_{24}^1 \\ p_{31}^1 & p_{32}^1 & p_{33}^1 & p_{34}^1 \\ p_{11}^2 & p_{12}^2 & p_{13}^2 & p_{14}^2 \\ p_{21}^2 & p_{22}^2 & p_{23}^2 & p_{24}^2 \\ p_{31}^2 & p_{32}^2 & p_{33}^2 & p_{34}^2 \\ \vdots \\ p_{11}^n & p_{12}^n & p_{13}^n & p_{14}^n \\ p_{21}^n & p_{22}^n & p_{23}^n & p_{24}^n \\ p_{31}^n & p_{32}^n & p_{33}^n & p_{34}^n \end{bmatrix} \begin{bmatrix} x \\ y \\ z \\ 1 \end{bmatrix} \quad (2.3)$$

and the $2n \times 1$ residue vector $r(X)$ of (2.2) can be written as in (2.4):

$$r(X) = \begin{bmatrix} p_{11}^{*1} & p_{12}^{*1} & p_{13}^{*1} \\ p_{21}^{*1} & p_{22}^{*1} & p_{23}^{*1} \\ p_{11}^{*2} & p_{12}^{*2} & p_{13}^{*2} \\ p_{21}^{*2} & p_{22}^{*2} & p_{23}^{*2} \\ \vdots \\ p_{11}^{*n} & p_{12}^{*n} & p_{13}^{*n} \\ p_{21}^{*n} & p_{22}^{*n} & p_{23}^{*n} \end{bmatrix} \begin{bmatrix} x \\ y \\ z \end{bmatrix} - \begin{bmatrix} u_1 - p_{14}^{*1} \\ v_1 - p_{24}^{*1} \\ u_2 - p_{14}^{*2} \\ v_2 - p_{24}^{*2} \\ \vdots \\ u_n - p_{14}^{*n} \\ v_n - p_{24}^{*n} \end{bmatrix} = AX - B = \begin{bmatrix} \phi_1(X) \\ \phi_2(X) \\ \phi_3(X) \\ \phi_4(X) \\ \vdots \\ \phi_{2n-1}(X) \\ \phi_{2n}(X) \end{bmatrix} \quad (2.4)$$

where $p_{l,m}^{*i} = \frac{p_{l,m}^i}{\lambda_i}$ ($\lambda_i = p_{3,1}^i x + p_{3,2}^i y + p_{3,3}^i z + p_{3,4}^i$, $i = 1, 2, \dots, n$, $l = 1, \dots, 3$, $m = 1, \dots, 4$).

Then cost function $f(X)$ in (2.2) has the equivalent least square problem form as in equation (2.1) [18] with $m = 2n$.

2.1 Symmedian point method for initialization

The fast two-view mid-point triangulation method [12, 13] has been extended to n -view cases by generalizing the concept *mid-point* into *symmedian point* which has the least sum of squared distances to all the projection rays. This idea was initially proposed by Sturm et al in 2006 [26], a simple and detailed implementation of which can also be found in [27, pp.305 ~ 307]. However, it seems the advantage of such method in initializing an L2 triangulation has not yet been sufficiently realized.

In 3D Euclidean space, a line l_i can be defined by a fixed point S_i and a direction W_i as:

$$l_i \triangleq \langle S_i, W_i \rangle \quad (2.5)$$

where W_i is a 3×1 unit direction vector with 2-norm equal to 1. Define the 3×3 projection P_i as:

$$P_i \triangleq I_{3 \times 3} - \frac{W_i W_i^T}{W_i^T W_i} = I_{3 \times 3} - W_i W_i^T \quad (2.6)$$

because the distance d_i between X and line $l_i = \langle S_i, W_i \rangle$ satisfies the quadratic form:

$$d_i^2 = \|P_i(X - S_i)\|_2^2 = (X - S_i)^T (P_i^T P_i) (X - S_i) \quad (2.7)$$

then the *symmedian point* \hat{X} which minimizes the sum of the n quadratic forms by (2.7) can be obtained by solving the 3×3 linear system of equations (2.8):

$$\left(\sum_{i=1}^n P_i \right) \hat{X} = \sum_{i=1}^n (P_i S_i) \quad (2.8)$$

This triangulation method requires pinhole camera factorization such that all projection rays can be represented into a fixed 3D point S_i and its direction W_i both in their Euclidean coordinates [27]. Such a multiple-view triangulation approach via *symmedian point* is linear, suboptimal and efficient. The *symmedian points* thus obtained in closed form usually are excellent initial values for further improvement in those two-stage triangulation methods [3, 24].

Note that the two-stage iterative methods find the L2 optimal solutions only when the initial triangulation locates the global-L2-optimal attraction basin of the problems correctly. However, it is difficult to clarify which initialization algorithm is in general better than others. It is in our extensive numerical experiments that we find *symmedian point* triangulation outperforms other linear triangulation methods and comparison details are omitted here. The iterative methods discussed in this work are all initialized by *symmedian points*, while the *tfml* method by Chesi et al [4] also works but is too much expensive.

2.2 Symbolic-numeric computation of derivatives

A symbolic-numeric approach is employed to compute accurate derivatives of (2.2). It because the subtle changes in the implementation of Newton-like iterative methods may causes significant difference in the numerical solutions to the general multiple-view triangulation why we present these implementation details in a separate subsection. In fact, this is probably one of the reasons why bundle adjustment optimization has long been considered as at most suboptimal even for Oxford VGG data sets besides no good initialization and the absence of optimality verification criterion [11].

Denote the $2n \times 3$ dimensional Jacobian matrix of $r(X)$ (2.4) as:

$$J(X) = \begin{bmatrix} \frac{\partial \phi_1}{\partial x} & \frac{\partial \phi_1}{\partial y} & \frac{\partial \phi_1}{\partial z} \\ \frac{\partial \phi_2}{\partial x} & \frac{\partial \phi_2}{\partial y} & \frac{\partial \phi_2}{\partial z} \\ \vdots & \vdots & \vdots \\ \frac{\partial \phi_{2n}}{\partial x} & \frac{\partial \phi_{2n}}{\partial y} & \frac{\partial \phi_{2n}}{\partial z} \end{bmatrix}_{2n \times 3} \quad (2.9)$$

Then the gradient g and Hessian H of the cost function $f(X)$ in (2.2) can be represented as [18]:

$$g(X) \triangleq \nabla f(X) = J(X)^T r(X) = J(X)^T (AX - B) \quad (2.10)$$

$$H(X) \triangleq \nabla^2 f(X) = J(X)^T J(X) + \sum_{i=1}^{2n} \phi_i \nabla^2 \phi_i \quad (2.11)$$

It is critical to assure appropriately high accuracy of $g(X)$ (2.10) since the least square problem is converted into solving a nonlinear system (2.12) using iterative methods. Any perturbation on $g(X)$, numerical round-off errors included, means using solutions of a perturbed system $\hat{g}(X) = 0$ to approximate

that of (2.12). Inappropriate approximation to derivatives may be one of the reasons why conventional implementation of iterative methods work unsatisfactory even for L2 triangulation problems close to the noise-free trivial cases.

$$g(X) = J(X)^T r(X) = J(X)^T (A X - B) = \mathbf{0} \quad (2.12)$$

The gradient (2.10) and Hessian (2.11) of reprojection error cost function (2.2) can be accurately estimated via a symbolic-numeric approach.

Considering the i -th partition of $r(X)$ as in (2.4), which consists of ϕ_{2i-1} and ϕ_{2i} corresponding to the i -th camera:

$$r_i(X) = \begin{pmatrix} \phi_{2i-1} \\ \phi_{2i} \end{pmatrix} = \begin{pmatrix} \frac{p_{11}^i x + p_{12}^i y + p_{13}^i z + p_{14}^i}{p_{31}^i x + p_{32}^i y + p_{33}^i z + p_{34}^i} - u_i \\ \frac{p_{21}^i x + p_{22}^i y + p_{23}^i z + p_{24}^i}{p_{31}^i x + p_{32}^i y + p_{33}^i z + p_{34}^i} - v_i \end{pmatrix} \quad (2.13)$$

Since both ϕ_{2i-1} and ϕ_{2i} are in rational forms and all such partitions are independent from each other, the first and second order partial derivatives of them and therefore the J (2.9), g (2.10) and H (2.11) can all be computed in a symbolic-numeric manner accurately.

For example, the i -th partition of $J(X)$ is:

$$J_i(X) = \begin{pmatrix} J_{2i-1} \\ J_{2i} \end{pmatrix} = \begin{bmatrix} \frac{\partial \phi_{2i-1}}{\partial x} & \frac{\partial \phi_{2i-1}}{\partial y} & \frac{\partial \phi_{2i-1}}{\partial z} \\ \frac{\partial \phi_{2i}}{\partial x} & \frac{\partial \phi_{2i}}{\partial y} & \frac{\partial \phi_{2i}}{\partial z} \end{bmatrix} \quad (2.14)$$

Denote $\lambda_i = p_{3,1}^i x + p_{3,2}^i y + p_{3,3}^i z + p_{3,4}^i$ and the following 18 determinants as:

$$\begin{aligned} 1) \Delta_{12}^{i,1} &= p_{11}^i p_{32}^i - p_{12}^i p_{31}^i, & 2) \Delta_{13}^{i,1} &= p_{11}^i p_{33}^i - p_{13}^i p_{31}^i, & 3) \Delta_{14}^{i,1} &= p_{11}^i p_{34}^i - p_{14}^i p_{31}^i, \\ 4) \Delta_{21}^{i,1} &= p_{12}^i p_{31}^i - p_{11}^i p_{32}^i, & 5) \Delta_{23}^{i,1} &= p_{12}^i p_{33}^i - p_{13}^i p_{32}^i, & 6) \Delta_{24}^{i,1} &= p_{12}^i p_{34}^i - p_{14}^i p_{32}^i, \\ 7) \Delta_{31}^{i,1} &= p_{13}^i p_{31}^i - p_{11}^i p_{33}^i, & 8) \Delta_{32}^{i,1} &= p_{13}^i p_{32}^i - p_{12}^i p_{33}^i, & 9) \Delta_{34}^{i,1} &= p_{13}^i p_{34}^i - p_{14}^i p_{33}^i, \\ 10) \Delta_{12}^{i,2} &= p_{21}^i p_{32}^i - p_{22}^i p_{31}^i, & 11) \Delta_{13}^{i,2} &= p_{21}^i p_{33}^i - p_{23}^i p_{31}^i, & 12) \Delta_{14}^{i,2} &= p_{21}^i p_{34}^i - p_{24}^i p_{31}^i, \\ 13) \Delta_{21}^{i,2} &= p_{22}^i p_{31}^i - p_{21}^i p_{32}^i, & 14) \Delta_{23}^{i,2} &= p_{22}^i p_{33}^i - p_{23}^i p_{32}^i, & 15) \Delta_{24}^{i,2} &= p_{22}^i p_{34}^i - p_{24}^i p_{32}^i, \\ 16) \Delta_{31}^{i,2} &= p_{23}^i p_{31}^i - p_{21}^i p_{33}^i, & 17) \Delta_{32}^{i,2} &= p_{23}^i p_{32}^i - p_{22}^i p_{33}^i, & 18) \Delta_{34}^{i,2} &= p_{23}^i p_{34}^i - p_{24}^i p_{33}^i \end{aligned} \quad (2.15)$$

let the Kronecker product of 3×3 identity matrix and $X^\ominus = (x, y, z, 1)^T$ be:

$$\text{Kron}(X^\ominus) = \begin{pmatrix} 1 & 0 & 0 \\ 0 & 1 & 0 \\ 0 & 0 & 1 \end{pmatrix} \otimes \begin{bmatrix} x \\ y \\ z \\ 1 \end{bmatrix} = \begin{pmatrix} X^\ominus & \mathbf{0} & \mathbf{0} \\ \mathbf{0} & X^\ominus & \mathbf{0} \\ \mathbf{0} & \mathbf{0} & X^\ominus \end{pmatrix}_{12 \times 3} \quad (2.16)$$

and the numerical part J_{num}^i of Jacobian's i -th partition independent of any variable x, y or z be:

$$J_{\text{num}}^i = \begin{pmatrix} 0 & \Delta_{12}^{i,1} & \Delta_{13}^{i,1} & \Delta_{14}^{i,1} & \Delta_{21}^{i,1} & 0 & \Delta_{23}^{i,1} & \Delta_{24}^{i,1} & \Delta_{31}^{i,1} & \Delta_{32}^{i,1} & 0 & \Delta_{34}^{i,1} \\ 0 & \Delta_{12}^{i,2} & \Delta_{13}^{i,2} & \Delta_{14}^{i,2} & \Delta_{21}^{i,2} & 0 & \Delta_{23}^{i,2} & \Delta_{24}^{i,2} & \Delta_{31}^{i,2} & \Delta_{32}^{i,2} & 0 & \Delta_{34}^{i,2} \end{pmatrix} \quad (2.17)$$

then $J(X)$'s i -th partition $J_i(X)$ as in (2.14) can be represented by:

$$J_i(X) = \begin{pmatrix} J_{2i-1} \\ J_{2i} \end{pmatrix} = J_{\text{num}}^i \text{Kron}(X^\ominus) * \lambda_i^{-2} \quad (2.18)$$

Note that no such numerical approximation as finite difference is needed when calculating the J (2.9) and then g (2.10) this way. The numerical parts J_{num}^i 's (2.17) of $J_i(X)$'s (2.18) can be pre-calculated since they only depend on the cameras. It is already enough with only the accurate J (2.9) and g (2.10) in the Gauss-Newton and Levenberg-Marquardt methods [18] where second order derivatives are unnecessary.

Accurate Hessian H (2.11) can also be obtained based on the accurate J per (2.18) and the analytical second order derivatives of (2.13) in similar way; and the first order finite-difference approximation to H (2.11) based on the accurate J (2.9) and g (2.10) also works well.

Per (2.11), we only need to further compute $\nabla^2 \phi_{2i-1}$ and $\nabla^2 \phi_{2i}$. Since both $\nabla^2 \phi_{2i-1}$ and $\nabla^2 \phi_{2i}$ are 3×3 symmetric matrices, each of them has only 6 independent entries. Number the 12 entries in the sequence as defined in (2.19), then every 6 of them can be rewritten into a 6×1 vector:

$$\text{indices of } \nabla^2 \phi_{2i-1} : \begin{bmatrix} 1 & 2 & 3 \\ 2 & 4 & 5 \\ 3 & 5 & 6 \end{bmatrix} \mapsto \begin{bmatrix} 1 \\ 2 \\ 3 \\ 4 \\ 5 \\ 6 \end{bmatrix}; \quad \text{indices of } \nabla^2 \phi_{2i} : \begin{bmatrix} 7 & 8 & 9 \\ 8 & 10 & 11 \\ 9 & 11 & 12 \end{bmatrix} \mapsto \begin{bmatrix} 7 \\ 8 \\ 9 \\ 10 \\ 11 \\ 12 \end{bmatrix} \quad (2.19)$$

All the 12 independent entries of $\nabla^2 \phi_{2i-1}$ and $\nabla^2 \phi_{2i}$ for the i -th camera can be concatenated together as one 12×1 dimensional column vector h_{12}^i , then be represented by the product of the following 12×4 matrix H_{num}^i and the homogeneous vector $(x, y, z, 1)^T * \lambda_i^{-3}$ (where: $\lambda_i = p_{31}^i x + p_{32}^i y + p_{33}^i z + p_{34}^i$):

$$H_{\text{num}}^i = \begin{pmatrix} 0 & 2p_{31}^i \Delta_{21}^{i,1} & 2p_{31}^i \Delta_{31}^{i,1} & 2p_{31}^i \Delta_{41}^{i,1} \\ p_{31}^i \Delta_{12}^{i,1} & p_{32}^i \Delta_{21}^{i,1} & p_{21}^i \Delta_{32}^{i,1} + p_{32}^i \Delta_{31}^{i,1} & p_{31}^i \Delta_{42}^{i,1} + p_{32}^i \Delta_{41}^{i,1} \\ p_{31}^i \Delta_{13}^{i,1} & p_{21}^i \Delta_{23}^{i,1} + p_{33}^i \Delta_{21}^{i,1} & p_{33}^i \Delta_{31}^{i,1} & p_{31}^i \Delta_{43}^{i,1} + p_{33}^i \Delta_{14}^{i,1} \\ 2p_{32}^i \Delta_{12}^{i,1} & 0 & 2p_{32}^i \Delta_{32}^{i,1} & 2p_{32}^i \Delta_{42}^{i,1} \\ p_{33}^i \Delta_{12}^{i,1} + p_{32}^i \Delta_{13}^{i,1} & p_{32}^i \Delta_{23}^{i,1} & p_{33}^i \Delta_{32}^{i,1} & p_{32}^i \Delta_{43}^{i,1} + p_{33}^i \Delta_{42}^{i,1} \\ 2p_{33}^i \Delta_{13}^{i,1} & 2p_{33}^i \Delta_{23}^{i,1} & 0 & 2p_{33}^i \Delta_{43}^{i,1} \\ 0 & 2p_{31}^i \Delta_{21}^{i,2} & 2p_{31}^i \Delta_{31}^{i,2} & 2p_{31}^i \Delta_{41}^{i,2} \\ p_{31}^i \Delta_{12}^{i,2} & p_{32}^i \Delta_{21}^{i,2} & p_{21}^i \Delta_{32}^{i,2} + p_{32}^i \Delta_{31}^{i,2} & p_{31}^i \Delta_{42}^{i,2} + p_{32}^i \Delta_{41}^{i,2} \\ p_{31}^i \Delta_{13}^{i,2} & p_{21}^i \Delta_{23}^{i,2} + p_{33}^i \Delta_{21}^{i,2} & p_{33}^i \Delta_{31}^{i,2} & p_{31}^i \Delta_{43}^{i,2} + p_{33}^i \Delta_{14}^{i,2} \\ 2p_{32}^i \Delta_{12}^{i,2} & 0 & 2p_{32}^i \Delta_{32}^{i,2} & 2p_{32}^i \Delta_{42}^{i,2} \\ p_{33}^i \Delta_{12}^{i,2} + p_{32}^i \Delta_{13}^{i,2} & p_{32}^i \Delta_{23}^{i,2} & p_{33}^i \Delta_{32}^{i,2} & p_{32}^i \Delta_{43}^{i,2} + p_{33}^i \Delta_{42}^{i,2} \\ 2p_{33}^i \Delta_{13}^{i,2} & 2p_{33}^i \Delta_{23}^{i,2} & 0 & 2p_{33}^i \Delta_{43}^{i,2} \end{pmatrix} \quad (2.20)$$

All the $\Delta_{mn}^{i,l}$'s are as those defined in equation (2.15). Then we can obtain accurate Hessian of $f(X)$ (2.2) per (2.11). Note that $\Delta_{12}^{i,l} = -\Delta_{21}^{i,l}$, $\Delta_{13}^{i,l} = -\Delta_{31}^{i,l}$, $\Delta_{23}^{i,l} = -\Delta_{32}^{i,l}$, $\forall l = 1, 2$.

2.3 Newton-like iterative methods and the globalizing strategies

Many state-of-the-art nonlinear optimizers can be used to minimize the unconstrained $f(X)$ (2.2). The classical Newton-like iterative methods, Newton-Raphson, Gauss-Newton and Levenberg-Marquardt methods, have locally superlinear and quadratic convergence rate [2, 7, 8, 18, 19, 21] when being initialized properly and therefore are our first choice.

The second order Taylor expansion of $f(X)$ around X_k gives rise to the quadratic model function $m_k^{NR}(d)$ and the Newton-Raphson step d_{k+1} , where the Newton step d_{k+1} is the minimizer of $m_k^{NR}(d)$ when $H(X_k)$ is positive definite:

$$\left\{ \begin{array}{l} f(X_k + d) \approx m_k^{NR}(d) = f(X_k) + d^T g(X_k) + \frac{1}{2!} d^T H(X_k) d \\ d_{k+1} = \arg \min_{d \in \mathbb{R}^3} m_k^{NR}(d) = -H(X_k)^{-1} g(X_k) \end{array} \right. \quad (2.21)$$

Similarly, the first order Taylor expansion of $r(X)$ (2.4) around X_k gives rise to the Gauss-Newton step s_{k+1} , the minimizer to another quadratic model function $m_k^{GN}(s)$ of $f(X)$ (2.2) around X_k :

$$\left\{ \begin{array}{l} r(X_k + s) \approx \hat{r}(s) = r(X_k) + J(X_k) s \\ m_k^{GN}(s) = \hat{r}(s)^T \hat{r}(s) = f(X_k) + 2s^T g(X_k) + s^T \left(J(X_k)^T J(X_k) \right) s \\ s_{k+1} = \arg \min_{s \in \mathbb{R}^3} m_k^{GN}(s) = - \left(J(X_k)^T J(X_k) \right)^{-1} g(X_k) = -J(X_k)^\dagger r(X_k) \end{array} \right. \quad (2.22)$$

Levenberg-Marquardt algorithm is considered as a modification on $J^T J$ in the Gauss-Newton iteration, or Gauss-Newton algorithm with trust region strategy on each step [7, 18].

$$p_{k+1} = - \left(J(X_k)^T J(X_k) + \mu_k I \right)^{-1} g(X_k) \quad (2.23)$$

The Levenberg-Marquardt algorithms we use are those from [9, 10, 18, 21, 30], with $\mu_k = \|r(X_k)\|_2^\delta$ ($\delta \in (1, 2)$) for the μ (2.23) updating in every iteration and is relatively expensive.

Algorithm 1 Soft line search with Armijo backtracking [14]

```

1: procedure SOFTLINESEARCH( $k, X_k, d_k, @f(X)$ ) ▷ modified Armijo backtracking
2:    $\gamma \leftarrow 0.01, \delta \leftarrow 0.25$  ▷ set the line search parameters:  $\gamma \in (0, 0.5), \delta \in (0, 1)$ 
3:    $i \leftarrow 0$  ▷ so as to compatible with the underlying iteration
4:   repeat ▷  $a \bmod b$ 
5:      $\alpha \leftarrow \delta^i$ 
6:      $\alpha_k \leftarrow \alpha$ 
7:     if  $f(X_k + \alpha * d_k) \leq f(X_k) - \gamma * \alpha^3 * \|d_k\|_2^3$  then ▷ Armijo backtracking criterion
8:       return  $\alpha_k$  ▷ return step length if meeting criterion
9:     end if
10:    increment  $i$  by 1
11:  until  $i \geq 20$ 
12:  return  $\alpha_k$  ▷ return after a max loop number
13: end procedure

```

The two major iterative approaches we suggest to use are Gauss-Newton hybrid with globalizing strategies 1 and 2: global Gauss-Newton [7, 18, 20, 21], denoted as *gGN* hereafter. The soft line search strategy with Armijo backtracking rule is as in algorithm 1, and simple trust region by Steihaug’s method is as in algorithm 2, the theoretically *local* convergence (to critical points of $f(X)$) of which have been depicted and proven in literatures [7, 17, 18, 20]. Unless otherwise specified, *gGN* represents Gauss-Newton with 1 in the numerical experiments.

Since without any globalizing strategy, the underlying Newton-Raphson and Gauss-Newton iterative methods work both accurate and efficient for more than 99% of the real cases, the globalizing strategies 1 and 2 better be hybrid with underlying Gauss-Newton iteration in a *smooth* manner. For example, a major difference between the trust region 2 version *gGN* and Levenberg-Marquardt is that trust region step-updating 2 is only implemented when the new $f_{k+1} = f(X_{k+1})$ is greater than $f_0 = f(X_0)$ in *gGN*, which makes the *gGN* more efficient without losing robustness. Too frequent trust region step-updating in Levenberg-Marquardt also ruins the accuracy according to our numerical experiments. Such hybridisation is also recommended to be used in the line search 1 version *gGN*.

Algorithm 2 Trust region algorithm: update s_k by conjugate gradient method

```

1: procedure TRUSTREGION( $g_k, B_k, X_k, @f(X)$ )                                ▷ simple trust region algorithm
2:    $i \leftarrow 0, x_i \leftarrow X_k, \epsilon \leftarrow 1.0e^{-8}, \Delta_i \leftarrow 1.0, \eta_s \leftarrow 0.1, \eta_v \leftarrow 0.9, \gamma_{\text{inc}} \leftarrow 4, \gamma_{\text{red}} \leftarrow 0.25$ 
3:   repeat
4:     model function:  $m_i(s) \leftarrow \left( -s^T g_k - \frac{1}{2} s^T B_k s \right)$   ▷ 2nd order Taylor exp:  $f(x_i) - f(x_i + s)$ 
5:      $s_i \leftarrow \arg \min_{\|s\|^2 \leq \Delta_i^2} m_i(s)$                                 ▷ solve subproblem by Steihaug method
6:      $\rho_i \leftarrow \frac{f(x_i) - f(x_i + s_i)}{m_i(s_i)}$                                 ▷ The ratio of actual to predicted reduction
7:     if  $\rho_i \geq \eta_v$  then                                                    ▷  $m_k(s)$  approximates  $f$  reduction very successful
8:        $x_{i+1} \leftarrow x_i + s_i$ 
9:        $\Delta_{i+1} \leftarrow \Delta_i * \gamma_{\text{inc}}$                                     ▷ increase trust region radius  $\Delta_i$ 
10:    else if  $\rho_i \geq \eta_s$  then                                                ▷  $m_k(s)$  approximates  $f$  reduction successful
11:       $x_{i+1} \leftarrow x_i + s_i$ 
12:       $\Delta_{i+1} \leftarrow \Delta_i$ 
13:    else                                                                      ▷  $m_k(s)$  does not approximate  $f$  reduction when  $\rho_i < \eta_s$ 
14:       $x_{i+1} \leftarrow x_i$ 
15:       $\Delta_{i+1} \leftarrow \Delta_i * \gamma_{\text{red}}$                                     ▷ reduce trust region radius  $\Delta_i$ 
16:    end if
17:    increment  $i$  by 1
18:  until  $\|g_i\| \leq \epsilon$  or  $i \geq 100$ 
19:  return  $s_k$ 
20: end procedure
    
```

Numerical experiments indicate that if accurate derivative computation in section 2.2 is used, all the Newton-like iterative methods initialized by *symmedian points* 2.1 are L2 optimal [4, 11] for most real cases. Here we use four synthetic data examples from Chesi et al [4] to illustrate the L2 optimality of the iterative methods, and the conservative case of *tfml* does not occur for any of the iterative methods at all.

Synthetic examples The synthetic data examples are based on the four cameras defined as in (2.24). The “SA2”, “SA3” and “SA4” examples are the cases with the first 2, 3 and 4 cameras as in (2.24) respectively and all their images are $(0, 0, 1)^T$. The conservative case “Con”, which *tfml* method fails in finding the optimal solution to, has the first three cameras and its 2D images are: $x_1 = (0.9, -0.9, 1)^T, x_2 =$

$(0.6, 2, 1)^T$, $x_3 = (2, 1.3, 1)^T$ respectively.

$$P_1 = \begin{bmatrix} 1 & 0 & 0 & 0 \\ 0 & 1 & 0 & 0 \\ 0 & 0 & 1 & 1 \end{bmatrix}, P_2 = \begin{bmatrix} -1 & -1 & -1 & 0 \\ 1 & 0 & -1 & 1 \\ 0 & 0 & 1 & 1 \end{bmatrix}, P_3 = \begin{bmatrix} 0 & -1 & 0 & 0 \\ 0 & 0 & -1 & 1 \\ -1 & -1 & 0 & 1 \end{bmatrix}, P_4 = \begin{bmatrix} 0 & -1 & -1 & 0 \\ 0 & 1 & -1 & 1 \\ 1 & 0 & 1 & 1 \end{bmatrix} \quad (2.24)$$

Comparison results are listed as in table 1. Since all the Newton-Raphson, Gauss-Newton and Levenberg-

Table 1: Triangulation results comparison between *tfml* and iterative methods

Exmp.	Method	Triangulation result	Reprojection error
SA2	<i>tfml</i>	(-0.2727272727272727 398 ,-0.1818181818181818 17941 ,0.6363636363636363 190)	0.0555555555555556
SA2	<i>gGN</i>	(-0.27272727272727273,-0.181818181818182,0.636363636363636)	0.0555555555555556
SA3	<i>tfml</i>	(-0.30250603 7933953 ,-0.160909 286697078 ,0.7990907 47348768)	0.105211035962143
SA3	<i>gGN</i>	(-0.302506061882800,-0.160909312731383,0.799090767385097)	0.105211035962142
SA4	<i>tfml</i>	(-0.232284 343064664 ,-0.334519 175175504 ,0.6968068 78848929)	0.209906166263281
SA4	<i>gGN</i>	(-0.232284268136407,-0.334519054968205,0.696806894375664)	0.209906166263248
Con	<i>tfml</i>	(1.314094728910344 ,- 1.106491029764633 , 0.043599248387159)	1.265349079248799
Con	<i>gGN</i>	(1.424098078272550,-1.238341159147880,0.115482211291935)	1.223123745015136

Marquardt methods perform similar, we only list the global Gauss-Newton (“gGN” with 1) results for comparison. Table 1 indicates that iterative methods are more accurate which also globally solves the conservative case for *tfml*. The L2 optimality can be easily verified by solving their (2.12) via global optimization methods or per the criterion ^[11] mentioned in section 2.4.

2.4 Numeric criteria in evaluating triangulation solutions

Because of their theoretical significance, there are global L2 optimality criteria developed by constructing the upper bound for $f(X)$ cost function or lower bound of its Hessian on a convex domain ^[5,6,11] based on *sufficient* conditions of the convexity. A *necessary and sufficient* criterion naturally generated from *tfml* and *tpml* algorithms using the equality of μ_1 and μ_2 is therefore of special interests ^[4] though it is only limited to the proposed algorithms’ verification. For those cases when camera number is small and when efficiency is not critical, it is also possible to compute all the real solutions to (2.12) and compare the corresponding reprojection errors.

Definition 2.1 (Numerical L2 optimality). A point is numerically L2 optimal if and only if it is a *good enough* approximate solution to the nonlinear normal equation (2.12) and its reprojection error is less than or equal to that of a *nice* suboptimal estimation easy to obtain.

The so-called *nice* suboptimal reprojection error can be the *upper local convexity level* as defined in ^[5,6] or simply use that of *symmedian point*, which works acceptable for most cases. The upper local convexity level is a sufficient criterion of L2 optimality but is rather difficult to compute accurately:

$$f_{LC} \triangleq \min_{X \in \mathbb{R}^3} \min_{y \in \mathbb{R}^3} \frac{y^T J(X)^T J(X) y}{\sum_{i=1}^{2n} (y^T \nabla^2 \phi_i(X) y)^2} \quad (2.25)$$

A more favorable efficient L2 optimality verification approach with high success ratio is the sufficient criteria via investigating the lower bounds of Hessian of $f(X)$ on the convex intersection set of n cone domains ^[11].

For the iterative methods proposed, we also use the following criteria to pre-determine whether the triangulation problem is a hard case or not, and the accuracy of a final solution.

Numerical experiments indicate that the square of an intrinsic curvature ρ of $r(X)$ around a specific point X works very well in picking out those hard cases, which is the reciprocal of the maximum eigen value λ_{\max} of symmetric matrix K (2.26) determined by using J^\dagger , the Moore-Penrose pseudo-inverse of J (2.9), and second order derivatives of $r(X)$ [7,8]:

$$K_{2n \times 2n}(X) \triangleq - \left(J^\dagger(X) \right)_{2n \times 3}^T \left(\sum_{i=1}^{2n} \phi_i(X) \nabla^2 \phi_i(X) \right)_{3 \times 3} J^\dagger(X)_{3 \times 2n} \quad (2.26)$$

The *intrinsic curvature* rule to determine the solvability via Gauss-Newton iteration of \hat{X}^* is as [7,8,22]:

$$\rho^2(\hat{X}^*) \triangleq \frac{1}{\lambda_{\max}^2(K(\hat{X}^*))} \geq \gamma^2(\hat{X}^*) \triangleq \|r(\hat{X}^*)\|_2^2 = f(\hat{X}^*), \quad (2.27)$$

$K(X)$ is as in (2.26), $f(X)$ is as in (2.2), and $r(X)$ is as in (2.4)

The the maximum absolute value of eigenvalues of K indicates the local convergence rate of Gauss-Newton iteration; and the maximum eigenvalue λ_{\max} of K (2.26), is useful to determine whether a least square problem is easily solvable via Newton-like iteration from a specific initialization. A rule of thumb useful in determine the solvability of an L2 triangulation problem by Newton-like iterative method proposed is whether ρ^2 is significantly larger than γ^2 at the symmedian point X_0 . The thumb rule also works for most of the global minimum determination when K_{LC} is smaller than ϵ and the reprojection error at a point \hat{X} is smaller than that of X_0 . Equation (2.27) indicates that, the larger residue it has at the initializer the more difficult a triangulation problem is for iterative methods to solve because of its nonlinearity and multiple local minima, which is verified in our numerical experiments on extensive data sets [1].

A quantitative criterion for accuracy estimation inspired by Kantorovich theorem [2,8] is the 2-norm of the iterative step at the current \hat{X} :

Definition 2.2 (LC distances). An estimation to the *local convergence* accuracy of \hat{X} , Kantorovich distance K_{LC} , is defined as:

$$K_{\text{LC}} = \left\| H(\hat{X})^{-1} g(\hat{X}) \right\|_2 \quad (2.28)$$

$K_{\text{LC}} \leq \epsilon \approx \sqrt{2.22 \times 10^{-16}} \approx 1.49 \times 10^{-8}$ for double precision computation usually means the current solution \hat{X} is a numerically good enough critical point of $f(X)$. The negative logarithm of K_{LC} also approximately indicate the accuracy of convergence in significant decimal digits.

3 Numerical Results for real data sets

Further numerical experiments are mainly conducted on the real data sets made available online by Oxford visual geometry group (<http://www.robots.ox.ac.uk/~vgg/data/data-mview.html>). Numerical results indicate that the L2 triangulation of all those data sets, *dinosaur*, *model house*, *corridor*, *Merton colleges I, II and III*, *University library* and *Wadham College*, can be globally solved by iteration methods (2.21) and (2.22) in high efficiency with or without globalizing strategies 1 and 2. Levenberg-Marquardt (2.23) only loses accuracy in very rare cases. The IEEE754 double precision C++ implementations of these iterative methods are conducted on a Windows® computer with a 3.4GHz Intel® i7 CPU.

Though global Gauss-Newton method (*gGN*), i.e., iteration (2.22) with Armijo backtracking line search strategy 1, is relatively slower than Newton-Raphson (2.21), it is more robust and therefore more favourable for general cases.

We present here comparison results between gGN and $tfml$ ^[4] on their ACT(average computing time) and R.E.(reprojection error) for the following data sets only: 1) *dinosaur* in table 2, which has the 21 camera case; 2) *corridor* in table 3, which has the $tfml$ conservative case (point No. 514); 3) *model house* in table 4, which has the maximum percentage of more than 4 camera cases. All indicate the iterative methods significantly outperform $tfml$ in both efficiency and accuracy.

Table 2: *dinosaur* data set results comparison between $tfml$ and global Gauss-Newton method

n	# points	ACT(s, $tfml$ ^[4])	ACT(s, gGN)	R.E.($tfml$ ^[4])	R.E.(gGN)
2	2300	0.010	0.0000362740	233.8453557	233.8453557
3	1167	0.048	0.0000408420	8073.5262739	8073.5262739
4	584	0.060	0.0000443918	14972.8533254	14972.8533254
5	375	0.071	0.0000477932	4450.9466754	4450.9466754
6	221	0.080	0.0000505274	10995.1067740	10995.1067739
7	141	0.097	0.0000521147	2955.3186392	2955.3186391
8	88	0.115	0.0000548824	5396.7423647	5396.7423646
9	44	0.148	0.0000574861	391.3195278	391.3195277
10	26	0.175	0.0000615819	222.4767185	222.4767185
11	15	0.215	0.0000737776	2930.4360400	2930.4360398
12	14	0.270	0.0000680938	62.3827050	62.3827049
13	5	0.303	0.0000799962	250.0569720	250.0569719
14	2	0.390	0.0000736568	9.5944806	9.5944806
21	1	1.094	0.0001041459	28.4078252	28.4078252
Total	4983	203.614	0.2051264558	50973.0136774	50973.0136765

Table 3: *corridor* data set results comparison between $tfml$ and global Gauss-Newton method

n	# points	ACT(s, $tfml$ ^[4])	ACT(s, gGN)	R.E.($tfml$ ^[4])	R.E.(gGN)
3	341	0.045	0.0000616368	94.4950818	94.4847897
5	146	0.078	0.0000655332	109.9579865	109.9579785
7	88	0.133	0.0000808400	135.1818406	135.1818014
9	58	0.220	0.0000968958	119.6534304	119.6533555
11	104	0.307	0.0001014581	204.1129585	204.1128521
Total	737	83.125	0.0538715274	663.4012979	663.3907772

First, from the tables 1 ~ 4, the conservative case for $tfml$ never occurred for gGN . Note that the “conservative case” for $tfml$ occurs only in *corridor* data set (point No.514), all other results by $tfml$ are $L2$ optimal per the criterion by Chesi et al ^[4]. By comparing the reprojection errors, it is easy to conclude that gGN results which are generally more accurate with smaller reprojection errors are also $L2$ optimal. The optimality of the gGN for the 3-view conservative case in *corridor* can be easily verified since which has been globally solven.

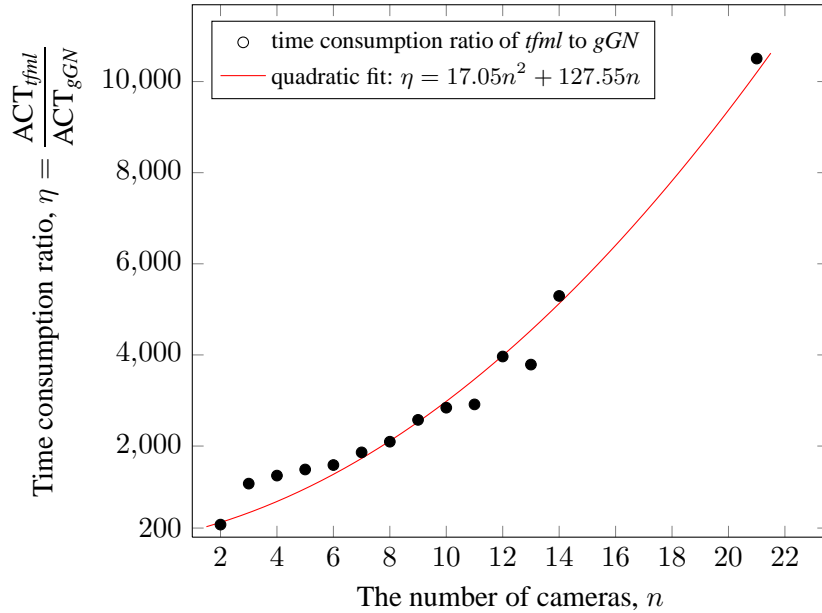
About efficiency, the three-view C++ implementation of gGN iteration are significantly faster than the C++ implementation of the three-view only $L2$ optimal methods ^[3, 16, 25]; both efficiency and reprojection

Table 4: *model house* data set results comparison between *tfml* and global Gauss-Newton method

n	# points	ACT(s, <i>tfml</i> ^[4])	ACT(s, <i>gGN</i>)	R.E.(<i>tfml</i> ^[4])	R.E.(<i>gGN</i>)
3	382	0.056	0.0000368079	146.9857377	146.9856478
4	19	0.083	0.0000921823	23.2842602	23.2842599
5	158	0.073	0.0000514310	538.8329042	538.8328594
6	3	0.089	0.0001322201	15.3877083	15.3877045
7	90	0.109	0.0000673846	304.2393664	304.2392904
8	1	0.172	0.0001234658	7.5343642	7.5343641
9	12	0.185	0.0001421567	63.4833436	63.4833353
10	7	0.230	0.0001360150	11.2098018	11.2097303
Total	672	48.582	0.03318089788	1110.9574864	1110.9571917

error of *gGN* are better than the the C++ implementation of the suboptimal methods by Recker et al ^[23,24].

There is a trend of the ACT ratio $\eta(n) = \frac{\text{ACT}_{tfml}}{\text{ACT}_{gGN}}$ between *tfml* and *gGN*: *tfml* becomes slow faster than *gGN* because its EVP scale is getting larger with the increase of camera number ^[4], as is illustrated in figure 1. For the 21-view case, *gGN*(C++) is more than 10000 times faster than *tfml*(per ACT in ^[4]).


 Figure 1: The trend of *tfml* to *gGN* time consumption ratio versus camera number (Oxford dinosaur data set)

Extensive numerical experiments are carried out based on the data sets by Agarwal et al ^[1], where radial distortions of the calibrated cameras are neglected for the purpose of algorithm verification. Iterative method *gGN* has only achieved L2 optimality for 99.7% of the points since there exist large residue cases or outliers. However, globalizing strategies 1 and 2 assure local convergence to critical points and significant reprojction error improvement of the *symmedian point* initializers for all those hard cases. And in such hard cases, neither iterative methods, nor *tfml* has absolute advantage over their peers; while *gGN* is the most

favourable method which has the overall robustness, high efficiency, higher success ratio of convergence to critical points and highest ratio of achieving the lowest reprojection error in such extensive numerical experiments.

4 Discussion and Conclusion

By symmedian point initialization and accurate computation of derivatives, Newton type iterative methods can solve most of the multiple view L2 triangulation problems both efficiently and accurately, which means the difficulty of the multiple local minima of the nonconvex reprojection error cost function $f(X)$ can be easily overcome in such real cases.

This indicate that *symmedian points* can efficiently locate the attraction basin of the optimal solution to $f(X)$ in most real cases which simplifies the multiple view L2 triangulation problem into convex ones, and accurate computation of derivatives are critical for Newton-like methods to be successful in solving multiple view L2 triangulation problem.

In order to handle those hard cases where the nonlinearity of $f(X)$ is so high and reprojection error is large at the initializers, globalizing strategies 1 and 2 are proposed to use smoothly-hybrid with the underlying Gauss-Newton iteration, which outperform Levenberg-Marquardt and other methods in robustness and efficiency, achieving high success ratio of convergence to critical points and significant reprojection error improvement over the symmedian point initializers.

This means bundle adjustment with appropriate implementations can significantly outperform its peers in solving optimal triangulation problems.

Similar to what has been proposed in ^[11], in the rare cases where *symmedian point* triangulation fails to locate the optimal solution attraction basin it is usually because the point has large noise, in which case in a large-scale reconstruction problem, the best option is probably to remove the point from consideration.

Future work on optimal triangulation may focus on improving initialization technique which assures to locate the attraction basin of the global minimum, while the problems of L2 optimality guaranteed triangulation for multiple view cases continue to be NP-hard with no simple solution in general ^[11]. And it is useful to develop efficient and reliable strategies, similar to the intrinsic normal curvature (2.27) for Gauss-Newton iterations, so as to previously determine whether a problem is solvable or not iteratively.

Acknowledgement

References

- [1] S. Agarwal, N. Snavely, S. M. Seitz, and R. Szeliski. Bundle adjustment in the large. In *Proceedings of the 11th European Conference on Computer Vision: Part II, ECCV'10*, pages 29–42, Berlin, Heidelberg, 2010. Springer-Verlag. Data sets are available from: <http://grail.cs.washington.edu/projects/bal/> (Accessed: Jan 15, 2014). (Cited on pages 10 and 12.)
- [2] I. K. Argyros. *Convergence and applications of Newton-type iterations*. Springer, New York, London, 2008. OHX. (Cited on pages 7 and 10.)
- [3] M. Byröd and K. Josephson. K.: Fast optimal three view triangulation. In *In: Asian Conference on Computer Vision*, 2007. (Cited on pages 1, 2, 4, and 11.)
- [4] G. Chesi and Y. S. Hung. Fast multiple-view L2 triangulation with occlusion handling. *Computer Vision and Image Understanding*, 115(2):211–223, Feb. 2011. (Cited on pages 1, 2, 4, 8, 9, 11, and 12.)
- [5] E. Demidenko. Is this the least squares estimate? *Biometrika*, 87(2):437–452, 2000. (Cited on page 9.)
- [6] E. Demidenko. Criteria for global minimum of sum of squares in nonlinear regression. *Computational Statistics & Data Analysis*, 51(3):1739–1753, Dec. 2006. (Cited on page 9.)

- [7] J. E. Dennis, Jr. and R. B. Schnabel. *Numerical Methods for Unconstrained Optimization and Nonlinear Equations*. Classics in Applied Mathematics, 16. Society for Industrial & Applied Mathematics, 1996. (Cited on pages 7, 8, and 10.)
- [8] P. Deuffhard. *Newton methods for nonlinear problems : affine invariance and adaptive algorithms*. Springer series in computational mathematics. Springer, Berlin, Heidelberg, New York, 2011. Autre tirage : 2006. (Cited on pages 7 and 10.)
- [9] J. Fan. The modified levenberg-marquardt method for nonlinear equations with cubic convergence. *Mathematics of Computation*, 81(277), 2012. (Cited on page 7.)
- [10] J.-y. Fan and Y.-x. Yuan. On the quadratic convergence of the levenberg-marquardt method without nonsingularity assumption. *Computing*, 74(1):23–39, Feb. 2005. (Cited on page 7.)
- [11] R. Hartley, F. Kahl, C. Olsson, and Y. Seo. Verifying global minima for L2 minimization problems in multiple view geometry. *International Journal of Computer Vision*, 101(2):288–304, Jan. 2013. (Cited on pages 1, 2, 4, 8, 9, and 13.)
- [12] R. I. Hartley and P. Sturm. Triangulation. *Computer Vision and Image Understanding*, 68(2):146–157, November 1997. (Cited on pages 1 and 3.)
- [13] R. I. Hartley and A. Zisserman. *Multiple view geometry in computer vision*. Cambridge University Press, Cambridge, UK, 2nd edition, 2003. (Cited on pages 2 and 3.)
- [14] F. Lampariello and M. Sciandrone. Global convergence technique for the newton method with periodic hessian evaluation. *Journal of Optimization Theory and Applications*, 111:341–358, 2001. (Cited on page 7.)
- [15] P. Lindstrom. Triangulation made easy. In *CVPR*, pages 1554–1561, 2010. (Cited on page 1.)
- [16] F. Lu and R. Hartley. A fast optimal algorithm for L2 triangulation. In *Proceedings of the 8th Asian conference on Computer vision - Volume Part II, ACCV’07*, pages 279–288, Berlin, Heidelberg, 2007. Springer-Verlag. (Cited on pages 1, 2, and 11.)
- [17] H. B. Nielsen and K. Madsen. *Introduction to Optimization and Data Fitting*. Informatics and Mathematical Modelling, Technical University of Denmark, DTU, Richard Petersens Plads, Building 321, DK-2800 Kgs. Lyngby, aug 2010. <http://www2.imm.dtu.dk/pubdb/p.php?5938> (Accessed Jan 1, 2014). (Cited on page 8.)
- [18] J. Nocedal and S. Wright. *Numerical optimization*. Springer series in operations research and financial engineering. Springer, New York, NY, 2. ed. edition, 2006. (Cited on pages 2, 3, 4, 6, 7, and 8.)
- [19] J. M. Ortega and W. C. Rheinboldt. *Iterative solution of nonlinear equations in several variables*. Computer science and applied mathematics. Academic Press, New York, 1970. (Cited on page 7.)
- [20] B. T. Poliak. *Introduction to optimization*. Translations series in mathematics and engineering. Optimization Software, Publications Division, 1987. (Cited on page 8.)
- [21] W. H. Press. *Numerical recipes 3rd edition: The art of scientific computing*. Cambridge university press, 2007. (Cited on pages 7 and 8.)
- [22] H. Ramsin and P.-Å. Wedin. A comparison of some algorithms for the nonlinear least squares problem. *BIT*, 17:72–90, 1977. (Cited on pages 2 and 10.)
- [23] S. Recker, M. Hess-Flores, and K. I. Joy. Fury of the swarm: Efficient and very accurate triangulation for multi-view reconstruction. In S. Recker and M. Hess-Flores, editors, *International Conference on Computer Vision Big Data 3D Computer Vision Workshop*, Dec. 2013. (Cited on pages 2 and 12.)
- [24] S. Recker, M. Hess-Flores, and K. I. Joy. Statistical angular error-based triangulation for efficient and accurate multi-view scene reconstruction. In S. Recker and M. Hess-Flores, editors, *Workshop on the Applications of Computer Vision (WACV)*, Jan. 2013. <http://www.thereckingball.com/triangulation.php> (Accessed: Jan 1, 2014). (Cited on pages 1, 2, 4, and 12.)
- [25] H. Stewénius, F. Schaffalitzky, and D. Nistér. How hard is 3-view triangulation really? In *IEEE International Conference on Computer Vision*, 2005. (Cited on pages 1, 2, and 11.)
- [26] P. Sturm, S. Ramalingam, and S. K. Lodha. On Calibration, Structure from Motion and Multi-View Geometry for Generic Camera Models. In K. Daniilidis and R. Klette, editors, *Imaging Beyond the Pinhole Camera*, volume 33 of *Computational Imaging and Vision*, pages 87–105. Springer, 2006. (Cited on page 3.)
- [27] R. Szeliski. *Computer Vision: Algorithms and Applications (Texts in Computer Science)*. Springer, 2011 edition, Oct. 2010. (Cited on pages 3 and 4.)

- [28] B. Triggs, P. F. McLauchlan, R. I. Hartley, and A. W. Fitzgibbon. Bundle adjustment - a modern synthesis. In *Proceedings of the International Workshop on Vision Algorithms: Theory and Practice*, ICCV '99, pages 298–372, London, UK, UK, 2000. Springer-Verlag. (Cited on page [2](#).)
- [29] F. C. Wu, Q. Zhang, and Z. Y. Hu. Efficient suboptimal solutions to the optimal triangulation. *International Journal of Computer Vision*, 91(1):77–106, 2011. (Cited on page [1](#).)
- [30] N. Yamashita and M. Fukushima. On the rate of convergence of the levenberg-marquardt method. *Computing*, (Suppl. 15):237–249, 2001. (Cited on page [7](#).)

Supplementary Materials

- A. Newton-like triangulator source codes in visual C++ for Windows platforms.
- B. Oxford visual geometry group data sets selected.